STUDYING NEUROLOGICAL IMPAIRMENT IN IL-10 GENE DEFICIENCY-INDUCED MOUSE COLITIS

by

MACKENZIE REESE NICHOLS

A thesis submitted in partial fulfillment of the
requirements for the degree of

MASTERS OF SCIENCE IN BIOLOGY

2025

Oakland University
Rochester, Michigan

Thesis Advisory Committee:

Dr. Sang Hoon Rhee, Ph.D., Chair
Dr. Zijuan Liu, Ph.D.
Dr. Elizabeth Delorme-Axford, Ph.D.

To my mother, father, and sister.

ACKNOWLEDGMENTS

I would like to thank all those who have supported me at Oakland University during my graduate and undergraduate studies. Most importantly, a tremendous thank you to my mentor, Dr. Sang Rhee, for the advice, trust, and knowledge granted to me during this project. I would also like to thank Dr. Zijuan Liu and Dr. Elizabeth Delorme-Axford for being a part of my thesis committee and guiding me through the completion of this project. Finally, the greatest thank you to my family for their unwavering support and encouragement with every crazy turn of events I brought our way. I would not be who I am today without you.

Mackenzie Reese Nichols

ABSTRACT

STUDYING NEUROLOGICAL IMPAIRMENT IN IL-10 GENE DEFICIENCY-INDUCED MOUSE COLITIS

by

Mackenzie Reese Nichols

Adviser: Dr. Sang Rhee, Ph.D.

Inflammatory Bowel Disease (IBD) is a group of diseases associated with chronic inflammation and mucosal immune responses within the gut. Elevated pro-inflammatory cytokines and chemokines drive this disease state, with loss of regulatory cytokines such as IL-10 exacerbating this response. The IL-10 Knockout (KO) mouse model replicates key pathological features of human IBD and provides an effective in vivo model for the study of intestinal inflammation and its systemic effects. Current research in the field highlights the link between IBD-associated inflammation and neurocognitive decline. CCL11 (eotaxin-1) is an age-related chemokine that has been linked to IBD, and is an emerging biomarker and mediator in neurocognitive decline due to its stimulation of reactive oxygen species (ROS). Experimental evidence shows that CCL11 easily crosses the blood-brain barrier (BBB), accumulates in regions associated with memory formation and retention, and consequently enhances ROS production via the interaction with microglial cells. This study investigates how intestinal inflammation amplifies ROS production in the brain through CCL11 signaling, using IL-10 KO mice, and highlights a link between IBD and neurocognitive decline.

TABLE OF CONTENTS

TABLE OF CONTENTS—Continued

LIST OF TABLES

LIST OF FIGURES

LIST OF ABBREVIATIONS

AD	Alzheimer's Disease
CCL1	C-C Motif Chemokine Ligand 1
CCL2	C-C Motif Chemokine Ligand 2
CCL8	C-C Motif Chemokine Ligand 8
CCL10	C-C Motif Chemokine Ligand 10
CCL11	C-C Motif Chemokine Ligand 11
CCL26	C-C Motif Chemokine Ligand 26
CCR3	C-C Chemokine Receptor 3
DMSO	Dimethyl Sulfoxide
IBD	Inflammatory Bowel Disease
IFN	Interferon
IL-1α	Interleukin 1-Alpha
IL-1β	Interleukin 1-Beta
IL-2	Interleukin 2
IL-6	Interleukin 6
IL-8	Interleukin 8
IL-10	Interleukin 10
IL-12	Interleukin 12
IL-17	Interleukin 17
IL-23	Interleukin 23
KO	Knockout
MS	Multiple Sclerosis

NOX-1	Nicotinamide Adenine Dinucleotide Phosphate Oxidase
PD	Parkinson's Disease
RIPA	Radio-Immunoprecipitation Assay Buffer
RLU	Relative Luminescence Units
ROS	Reactive Oxygen Species
RPM	Revolutions Per Minute
TNF	Tumor Necrosis Factor

CHAPTER ONE

INTRODUCTION

Inflammatory bowel disease (IBD) is a class of chronic inflammatory diseases associated with severe inflammatory responses within the gastrointestinal tract's epithelial lining, lamina propria, and submucosa. There are two clinical manifestations of IBD: Ulcerative colitis and Crohn's disease. Bassaganya-Riera et al. (2010) stated that IBD is most accompanied by recurring diarrhea, rectal bleeding, and signs of malnutrition as lesions in the epithelial layer progress and allow bacteria to enter the lamina propria. At lesion sites, bacterial antigens are picked up by antigen-presenting cells, including dendritic cells and macrophages, which then transport the antigen into the lamina propria. This causes the continuation of the inflammatory cascade in the gastrointestinal tract, due to more antigen-presenting cells being chemotactically signaled to the area. Pro-inflammatory cytokines such as IL-1α, IL-1β, IL-2, -6, -8, -12, -17, -23, IFN, and TNF are regularly expressed in the constant mucosal immune response within the gastrointestinal tract (Műzes et al., 2012). Additionally, chemokines such as CCL2 (MCP-1), CCL11 (Eotaxin-1), CCL26 (Eotaxin-3), CCL1 (I-309), CXCL8 (IL-8), and CXCL10 (IP-10) have been identified as key biomarkers of IBD (Song et al., 2024). All of which are pro-inflammatory and are associated with chronic inflammatory states, autoimmune diseases, and allergic responses.

On the other hand, interleukin 10 (IL-10) is a potent anti-inflammatory cytokine contributing to the regulation of the immune system. This interleukin is essential in protecting the mucosal immunogenic responses within the gut and overall homeostasis by downregulating the production of Th1-derived cytokines (Li, 2004). The loss of IL-10

can lead to excessive immune responses within the gut and the subsequent development of spontaneous IBD. The IL-10 Knockout (KO) mouse model is a well-studied murine model for IBD that develops spontaneous intestinal inflammation or is induced upon cycles of Piroxicam. As referenced in the study by Kim et al., (2023) the IL-10 KO mouse model is characterized by histological parameters similar to that of human IBD with inflammatory infiltrates influencing the lamina propria and submucosa; leading to epithelial hyperplasia, mucin depletion, ulcers, and visible thickening of the intestinal wall of the small intestine and colon. This mouse model is an ideal candidate for studying the connection between intestinal inflammation and its potential impacts on secondary locations within the body.

The gut-brain axis, encompassing the gastrointestinal tract and the central nervous system, is a growing area of study linked to the prevalence of neurological conditions. Due to medical advancements, public health measures, disease eradication methodologies, and a variety of other factors, humans are living longer than ever. Because of this, the prevalence of neurological disease is becoming more prevalent, especially amongst the aging population. According to McDonald (2017), the increase in the prevalence of neurodegenerative disease doubles every 20 years, with the predicted incidence of dementia being 115 million people worldwide by 2050. Other age-related neurological disorders include Alzheimer's disease (AD), Multiple Sclerosis (MS), and Parkinson's disease (PD). Systemic inflammation caused by IBD has been linked to degradation of the blood-brain barrier, neuroinflammation, and the potential to exacerbate dysfunction in the brain with an emphasis on the hippocampal and cerebellar regions (Çalıkuşu et al., 2024). Additionally, studies have linked IBD as a pathogenic risk factor

to AD, PD, and MS, with potential shared mechanisms still not yet fully understood (Zhu et al, 2022; Günther et al., 2021; Zhang et al., 2021). One of the driving factors of these inflammatory states is the upregulation of reactive oxygen species (ROS), which are natural byproducts of cellular metabolism; however, in excess, they cause damage to cellular DNA, RNA, lipids, and proteins. Elevated levels of ROS have been viewed in many different human diseases, including those previously stated: Alzheimer's Disease, Parkinson's Disease, and Multiple Sclerosis. Oxidative stress due to excess ROS has been linked as a major mechanism of neurocognitive disease advancement (Akbar et al., 2016). A cellular culprit for the production of ROS within the brain is microglial cells, which are responsible for the development and maintenance of neurons. The stimulation of microglial cells via C-C motif chemokine 11 (CCL11, also known as eotaxin-1), which binds to the microglial CCR3 receptor, upregulates the production of ROS within the brain.

In the research study conducted by Horiuchi et al. (2015), it was found that astrocytes within the brain are primarily responsible for the release of CCL11 and lead to elevated levels of CCL11 within the cerebrospinal fluid. Whereas, microglia express the CCL11 receptor (CCR3), which upregulates NOX-1 (NADP-oxidase 1), leading to the greater conversion of oxygen to superoxide species. Therefore, promoting excitotoxic neuronal death within the brain due to oxidative stress caused by ROS (Horiuchi et al., 2015). The study was able to make numerous conclusions regarding the effects of CCL11 on pathways within the brain; however, the study was based on cell cultures with glutamate to induce glutamate-mediated neuronal cell death. Accordingly, the harmful effect of CCL11 on the brain remains elusive.

As discussed by Sirivichayakul et al. (2019), peripheral CCL11 is also transported through the blood-brain barrier and accumulates in brain regions. It also refers to the idea that "eotaxin could be an independent predictor of cognitive impairment in older individuals" (Sirivichayakul et al., 2019). Although this study makes no mention of ROS in its findings, it does heavily discuss mental and cognitive symptoms that may arise in individuals with elevated CCL11 levels. Making further research into this chemokine scientifically significant for the aging population. The ability of the CCL11 chemokine to cross the blood-brain barrier raises the question of the effects of peripheral CCL11 on various cell types within the brain. The mechanism by which CCL11 is up taken into the brain was studied by Banks et al. (2014) through the analysis of injected CCL11 and its ability to cross the blood-brain barrier of CD-1 mice. Through this study, CCL11 uptake demonstrated a slow uptake phase for the first 15 minutes, followed by a rapid phase uptake for the remainder of the testing time frame of 60 minutes. The outcome of this study concluded that this rapid influx of CCL11 for the majority of the testing phase and slow efflux supports the accumulation of this chemokine in the central nervous system when present in serum in excess. It was also able to isolate brain regions with the highest levels of CCL11 uptake, including the basal ganglia and the hypothalamus, having the most rapid uptake (Banks et al., 2014). Drawing significance to the effects of peripheral CCL11 due to the prominent uptake and subsequent impact it may have upon neurocognitive function. The direct impacts of peripheral CCL11 on memory and cognitive function remain unknown.

Although CCL11 does serve a vital role in the immune system and the regulation of inflammatory responses, the natural increase of this chemokine with age and under

certain inflammatory disease states calls into question the role it may have on neurocognitive decline. Circulating CCL11 in the bloodstream has the potential to be up taken and retained within the brain, leading to unknown molecular mechanisms that induce the production of reactive oxygen species by microglial cells. This study will investigate the link between Inflammatory Bowel Diseases, the role that C-C Motif Chemokine Ligand 11 (CCL11) plays in the stimulation of microglial cells to produce reactive oxygen species, as well as explore the underlying neurocognitive effects that this biological process has upon the brain. We hypothesize that intestinal inflammation will increase ROS production within the brains of IL-10 knockout mice and lead to evident neurocognitive decline.

CHAPTER TWO

METHODOLOGY

To test that CCL11 stimulates microglial cells to produce ROS in the brain, we will treat SIM-A9 cell cultures with various levels of CCL11 for 8 hours. SIM-A9 is a microglial cell line derived from the cerebral cortexes of mouse pups and provides an effective way to study microglial cells in vitro. SIM-A9 will be plated and allowed to proliferate until the density of cells is high, with ~80% plate coverage. After a media change with DMSO (10% Fetal Bovine Serum, 1% Penicillin Streptomycin), the cells will then be treated with CCL11 at a quantity ranging from 12.5-200 ng/mL, and then placed to incubate for 8 hours along with untreated controls. Using CCL11 at this range of doses will allow for the determination of an efficacious dose and give insight into the mechanism by which CCL11 activates microglial cells. Once the 8-hour incubation period has been completed, the cell lysates and cell supernatant will be evaluated for ROS production by using the ROS- GLO^{TM} H_2O_2 Assay by Promega and an illuminator that measures the fluorescence of each sample.

To test the effects of serum CCL11 on neurocognitive function, IL-10 knockout and control C57BL/6 age-matched mice will undergo three cycles of piroxicam to induce intestinal colitis. Taking their weight daily will be used as an indicator of colitis. Upon the completion of the third cycle of piroxicam, the mice will undergo rota-rod and passive avoidance training and testing. These mice will then be euthanized and harvested for physical and biological analysis. Hippocampal and cerebral tissue samples will be analyzed for ROS production using the ROS-GLO^{TM} H_2O_2 Assay by Promega and an

illuminator that measures the fluorescence of each sample. The colons of these mice will also be collected and measured to identify the degree of colitis presence and ensure visible inflammation and shortening in colitis states.

CELL CULTURE

Using homogeneous DMEM medium treated with 10% fetal bovine serum and 1% penicillin-streptomycin, stock Sim-A9 cells were cultured in sterile petri dishes and allowed to proliferate until their confluency was approximately 80%. During the duration of this growth period, the cells were incubated at 37 °C with 5% CO_2, while their growth was monitored under a microscope, with routine medium changes every 2-3 days depending on the coloration of the media. Sterile conditions were maintained and practiced for the entirety of the growth phase, and no notable signs of contamination were observed in the cultures used in this experiment.

To investigate the underlying cellular and molecular mechanisms behind microglial cells' interactions with CCL11, Petri dishes 1 - 6 of SIM-A9 cells with confluency of ~80% were treated with the following CCL11 quantities respectively: 0 ng/mL (Control), 12.5 ng/mL, 25 ng/mL, 50 ng/mL, 100 ng/mL, and 200 ng/mL. These cultures were then allowed to incubate at 37 °C with 5% CO_2 for exactly 8 hours. After this period, the cell lysates and supernates (cell medium) were harvested and placed in the -80 °C freezer for storage until the testing of Reactive Oxygen Species could be performed. Cell lysates were prepared in a RIPA (radioimmunoprecipitation assay) buffer, which allows for the rapid lysis and extraction of cellular contents, before freezing.

ANIMALS

Adult male and female homozygous IL-10 -/- (IL-10-KO) and C57BL/6 (wild type/IL-10-WT) mice will be purchased from Jackson Laboratories and housed in Oakland University's accredited animal facilities. These mice will be maintained in a specific pathogen-free environment under barrier-protected conditions with a standard 12h/12h light and dark cycle. Mice will be housed at a maximum of 4 animals per cage and consume a standard chow diet of 20% calories from protein, 3 % from fat, and 77 % from carbohydrates. This study is approved by Oakland University's Institutional Animal Care and Use Committee (IACUC Protocol 2022-1183). Animals were allowed to age to 2 months before undergoing any experimental protocol.

Three cycles of piroxicam-treated chow (240 ppm piroxicam food) will be used for both IL-10 -/- and control C57BL/6 mice in a cycle of six days on treatment diet, 6 days on regular chow diet for a total of three treatment cycles. Upon completion of the last cycle of piroxicam, mice will immediately undergo Rota-Rod training and testing to indicate their grip strength and neuromuscular coordination. Mice will undergo training for 60 seconds at 30 revolutions per minute (RPM). During the training phase, if mice are to fall, they will be returned to the apparatus until their 60 seconds are complete. Upon the completion of training, mice will be allowed five minutes to rest in normal housing conditions before being tested on the Rota-Rod apparatus for a maximum allotted time of 300 seconds at 30 RPM, recording the time of their fall off the spinning rod in seconds. Reduced times are an indicator of decreased muscle strength or potential abnormalities in neuromuscular coordination.

After an additional 24 hours of rest, mice will begin passive avoidance training and testing. This testing protocol is used to test memory strength in combatants of natural instinct over 7 days. On day zero, mice are placed in a light chamber and allowed to freely move from the light chamber to one that is dark. A trap door between the two spaces closes, and a negative stimulus of 0.2 mA is delivered to the paws of the mice in the dark chamber for 30 seconds. The mouse is then placed in normal housing conditions for 5 minutes before undergoing day 0 testing. Testing occurs on days 0, 1, 3, and 7 for a maximum of 300 seconds (5 minutes). The same light and dark chamber is set up without an electric field in the dark chamber. As demonstrated by Figure 1, a mouse is placed in the light chamber, while observers measure the time that elapses before moving into the dark chamber. Decreases in elapsed time before moving from the light to dark chamber from day 0 to day 7 indicate long-term memory decline.

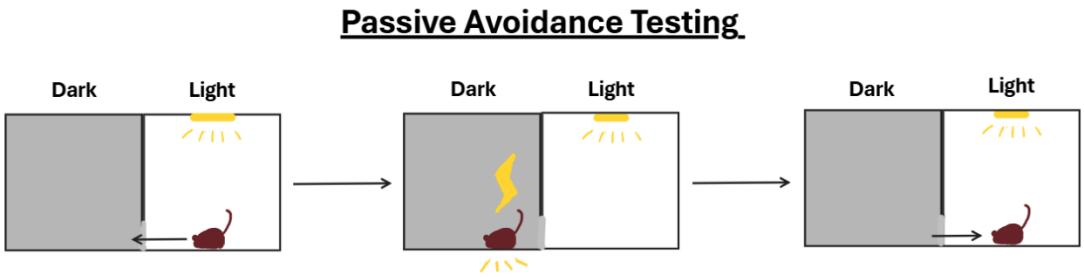

Figure 1: *A representative image of passive avoidance testing in mice. On day 0, while training, the dark chamber has the addition of an electric field of 0.2mA running through the base, triggered by the mouse's entry. All testing phases do not have a current running through the base of the dark chamber.*

Upon the completion of behavioral and memory testing, the mice will be euthanized for the collection of tissue samples. Brain tissue samples, including the cerebrum and hippocampus, will be collected and homogenized in complete RIPA (10 mL RIPA Buffer, 50 µL phosphatase inhibitor cocktail, and 1 tablet complete protease inhibitor cocktail) buffer. Samples will be left on ice for one hour after homogenizing, then spun down in a centrifuge at 4 °C at 14,000 rpm for 10 minutes. The liquid suspension will then be aliquoted to fresh microcentrifuge tubes and stored in a -80 °C freezer for later testing.

ROS-GLO™ H_2O_2 ASSAY

With the ROS-GLO™ H_2O_2 assay, luminescence from the presence of hydrogen peroxide in each sample was obtained using an illuminator and recorded as a maximum relative luminescence units per second. All samples were taken from the -80 °C freezer and placed on ice to warm at a steady pace. Contents of the ROS-GLO™ H_2O_2 assay were also placed on ice to thaw. To form the H_2O_2 Substrate Solution, we will combine 5 µL of H_2O_2 substrate and 400 µL of dilution buffer in an Eppendorf tube and store it on ice. After adding 60 µL of each resuspended sample into marked Eppendorf tubes, we then added 15 µL of the substrate solution into each testing sample. Each Eppendorf now had a sample volume of 75 µL, and lights were turned off for the remainder of the experiment. We then formed the ROS-GLO™ Detection Solution by combining 2.5 mL of luciferin detection agent, 25 µL of D-cystine, and 25 µL of signal enhancer, then vortexed to make a homogenous mixture. Then, 75 µL of the detection solution was added to each Eppendorf tube containing the 75 µL of the sample, with a 60-second

interval between each addition to allow for the testing of samples after the 20-minute wait between addition and testing.

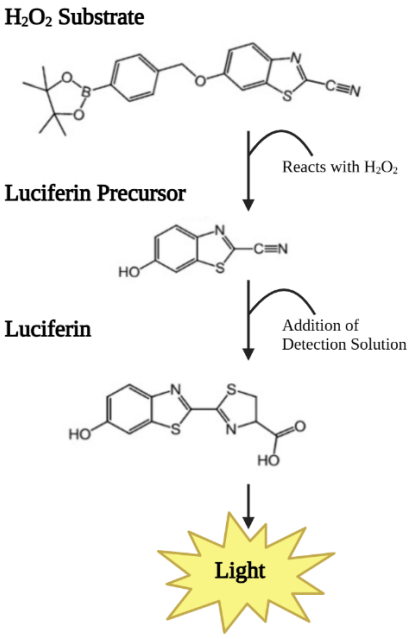

Figure 2: *Mechanism for the detection of H_2O_2 by the ROS-GLO^{TM} H_2O_2 Assay. Figure hand drawn in the free version of BioRender (Duellman, 2013).*

After the 20-minute wait time from the first addition of the detection solution, we processed each sample through an illuminator and recorded the maximum fluorescence of each sample for 30 seconds, and allocated 30 seconds for recording and the sample changing process (60 seconds total between tested samples). By this detection method, the H_2O_2 substrate reacts with the presence of H_2O_2 to produce the luciferin precursor. Upon addition of the ROS-GLO^{TM} Detection Solution, the precursor is converted to luciferin, which reacts with the recombinant luciferase to generate a luminescent signal proportional to the H_2O_2 concentration (Duellman, 2013). A luminator is used to quantify the amount of light emitted from each sample in relative light units per second (RLU/s).

STATISTICAL ANALYSIS

All statistical analysis were performed using Microsoft Excel (Version 2509, Microsoft Corporation, Redmond, WA, USA). Descriptive statistics, including means, variance, and standard deviation, were calculated for all measured variables to summarize the dispersion of the data. T-tests were conducted to compare differences between two independent groups and data was analyzed using two-tailed t-tests with unequal variances. All T-tests were performed at a 95% confidence level ($p < 0.05$). Excel's built in data-analysis tool pack was used to calculate t-statistics and corresponding p-values, and statistically significant outcomes are noted throughout the results section.

CHAPTER THREE

RESULTS

CELL CULTURE - H_2O_2 QUANTIFICATION

Name of Sample	Cell Supernatant (RLU/s)	Cell Lysate (RLU/s)
SIM-A9- 0 ng/mL CCL11 - Sample 1 (Petri dish 1)	96,345	206,739
SIM-A9- 0 ng/mL CCL11- Sample 2 (Petri dish 1)	108,457	299,000
SIM-A9-12.5 ng/mL CCL11 - Sample 1 (Petri Dish 2)	72,000	252,672
SIM-A9-12.5 ng/mL CCL11- Sample 2 (Petri Dish 2)	65,000	198,203
SIM-A9-25 ng/mL CCL11 - Sample 1 (Petri Dish 3)	107,024	199,620
SIM-A9-25 ng/mL CCL11 - Sample 2 (Petri Dish 3)	145,550	287,873
SIM-A9- 50 ng/mL CCL11 - Sample 1 (Petri Dish 4)	178,411	360,004
SIM-A9- 50 ng/mL CCL11 - Sample 2 (Petri Dish 4)	126,043	299,870
SIM-A9-100 ng/mL CCL11- Sample 1 (Petri Dish 5)	172,000	257,000
SIM-A9 - 100 ng/mL CCL11- Sample 2 (Petri Dish 5)	109,030	297,742
SIM-A9 - 200 ng/mL CCL11 - Sample 1 (Petri Dish 6)	133,478	351,420
SIM-A9- 200 ng/mL CCL11 - Sample 2 (Petri Dish 6)	120,746	246,000

Table 1A: *Maximum RLU of H_2O_2 Values from SIM-A9 Microglial Cells Stimulated by CCL11 during day 1 of testing. A notable difference in RLU/s values between supernatant and cell lysate. Cell Lysate has higher quantities of H_2O_2, representing intracellular ROS production under normal and stimulated conditions.*

RLU values from trial 2 of only Supernatant:

Name of Sample	Cell Supernatant (RLU/s)
SIM-A9- 0 ng/mL CCL11 - Sample 3 (Petri dish 1)	65,556
SIM-A9- 0 ng/mL CCL11- Sample 4 (Petri dish 1)	77,880
SIM-A9-12.5 ng/mL CCL11 - Sample 3 (Petri Dish 2)	83,880
SIM-A9-12.5 ng/mL CCL11- Sample 4 (Petri Dish 2)	98,750
SIM-A9-25 ng/mL CCL11 - Sample 3 (Petri Dish 3)	94,997
SIM-A9-25 ng/mL CCL11 - Sample 4 (Petri Dish 3)	116,138
SIM-A9- 50 ng/mL CCL11 - Sample 3 (Petri Dish 4)	90,008
SIM-A9- 50 ng/mL CCL11 - Sample 4 (Petri Dish 4)	99,587
SIM-A9-100 ng/mL CCL11- Sample 3 (Petri Dish 5)	103,100
SIM-A9 - 100 ng/mL CCL11- Sample 4 (Petri Dish 5)	114,697
SIM-A9 - 200 ng/mL CCL11 - Sample 3 (Petri Dish 6)	113,570
SIM-A9- 200 ng/mL CCL11 - Sample 4 (Petri Dish 6)	132,139

Table 1B: *Maximum RLU of H_2O_2 Values from SIM-A9 Microglial Cells Stimulated by CCL11 during the 2nd day of testing. Cell Supernatants are correlated to the release of H_2O_2 into cell culture media in response to stimulation.*

RLU values from trial 3 of only Supernatant:

Name of Sample	Cell Supernatant (RLU/s)
SIM-A9- 0 ng/mL CCL11 - Sample 5 (Petri dish 1)	76,331
SIM-A9- 0 ng/mL CCL11- Sample 6 (Petri dish 1)	79,863
SIM-A9-12.5 ng/mL CCL11 - Sample 5 (Petri Dish 2)	87,440
SIM-A9-12.5 ng/mL CCL11- Sample 6 (Petri Dish 2)	78,872
SIM-A9-25 ng/mL CCL11 - Sample 5 (Petri Dish 3)	91,217
SIM-A9-25 ng/mL CCL11 - Sample 6 (Petri Dish 3)	118,688
SIM-A9- 50 ng/mL CCL11 - Sample 5 (Petri Dish 4)	114,113
SIM-A9- 50 ng/mL CCL11 - Sample 6 (Petri Dish 4)	100,883
SIM-A9-100 ng/mL CCL11- Sample 5 (Petri Dish 5)	119,872
SIM-A9 - 100 ng/mL CCL11- Sample 6 (Petri Dish 5)	106,731
SIM-A9 - 200 ng/mL CCL11 - Sample 5 (Petri Dish 6)	124,99
SIM-A9- 200 ng/mL CCL11 - Sample 6 (Petri Dish 6)	135,670

Table 1C: *Maximum RLU of H_2O_2 Values from SIM-A9 Microglial Cells Stimulated by CCL11 during the 3rd day of testing. Cell Supernatants are correlated to the release of H_2O_2 into cell culture media in response to stimulation.*

As seen in the data tables 1A-C, the production of H_2O_2 in cell supernatant vs. cell lysate greatly differs. Detected luminescence is directly proportional to the quantity of H_2O_2 in solution, with the negative control of 0 ng/mL of CCL11 demonstrating the natural occurrence of H_2O_2 produced by these cells in vitro. It is seen in all data tables

that with the increased treatment of CCL11, there is also a corresponding increase in H_2O_2 production. The ROS-GLO^{TM} H_2O_2 Assay can screen for the presence of H_2O_2, not any of the other superoxide species: hydroxyl radical, hydroxide ion, triplet oxygen, superoxide anion, peroxide ion, and nitric oxide. Superoxide species are converted by superoxide dismutase to H_2O_2, and then converted by catalase or glutathione peroxidase to H_2O in normal cellular responses. It should also be noted that there was visible cell death in the samples treated with 100 ng/mL and 200 ng/mL of CCL11 after the 8-hour treatment period in comparison to the others.

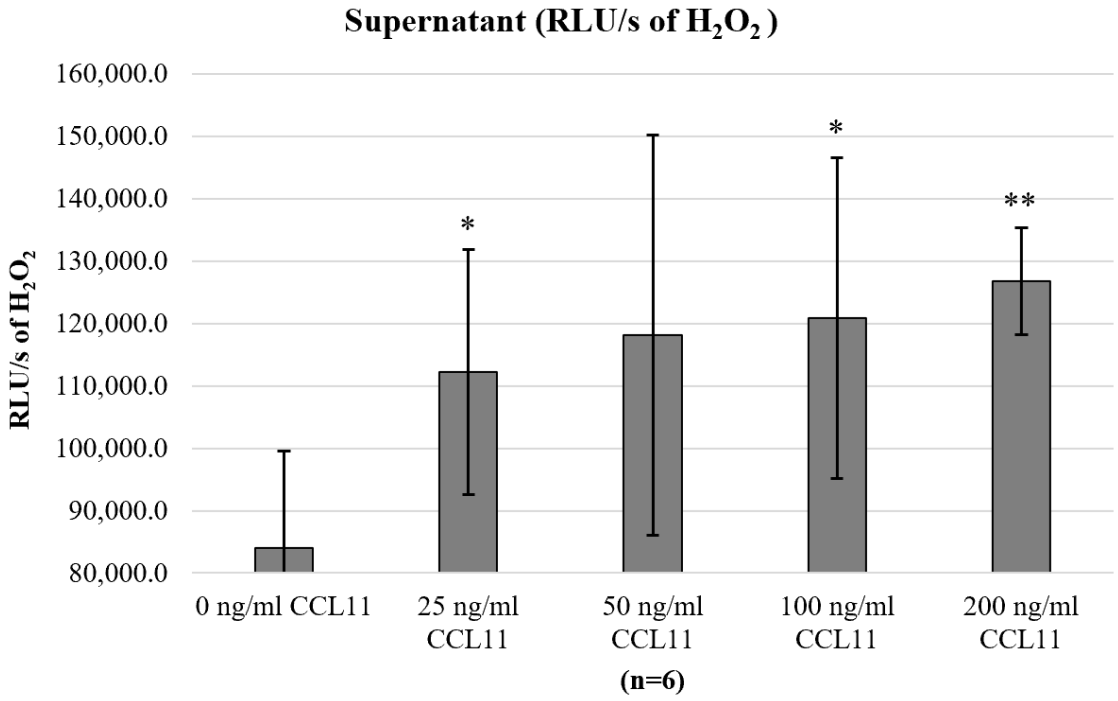

Figure 3A: *All collected Supernatant Data in RLU/s of H_2O_2 Vs the amount of CCL11 stimulation in ng/mL. This directly corresponds to the quantity of H_2O_2 released into the cell culturing medium by SIM-A9 microglial cells in response to CCL11 treatment. 0-25 ng/ml, 0-100 ng/ml p-value <0.05. 0-200 ng/ml p-value <0.001.*

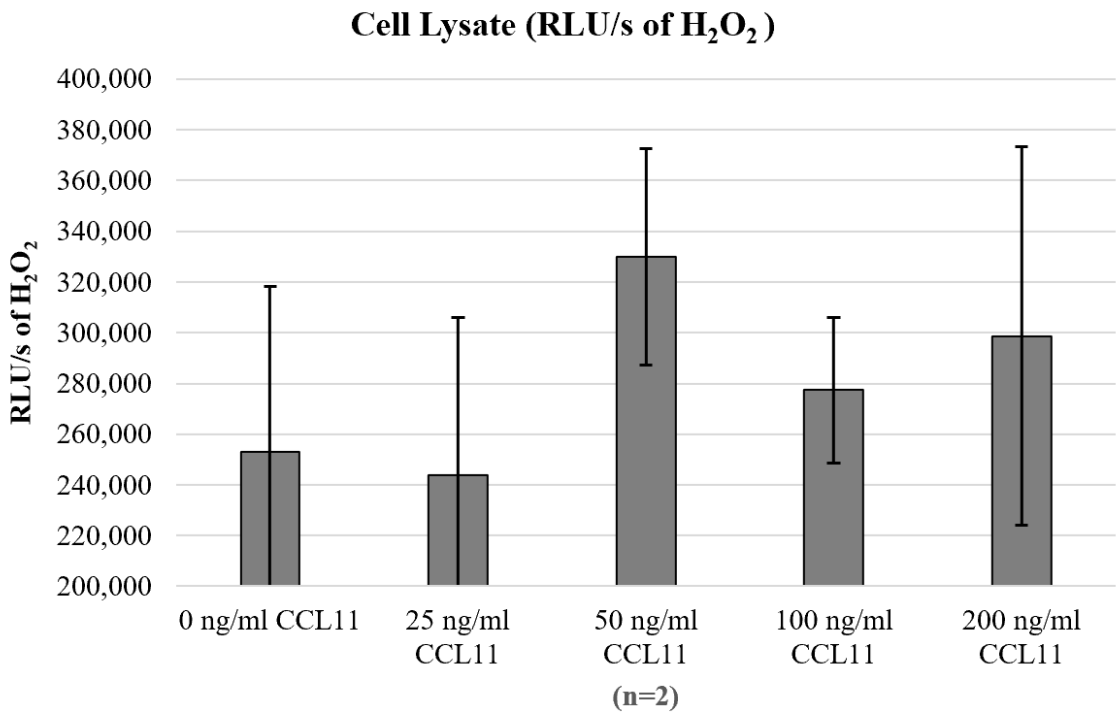

Figure 3B: *All collected Cell Lysate Data in RLU/s of H_2O_2 vs the amount of CCL11 stimulation in ng/mL. This directly corresponds to the quantity of H_2O_2 in each sample produced within SIM-A9 microglial cells in response to CCL11 treatment. No statistical data calculated n=2. Significant cell death visible for samples treated with 100-200ng/ml CCL11.*

From the data plotted in Figures 2A and 2B, the average luminescence recorded (RLU/s) is plotted in correspondence to the treatment (0 ng/mL (Control), 25 ng/mL, 50 ng/mL, 100 ng/mL, and 200 ng/mL). Standard deviation for each sample set is shown as the error bars on each graph. Statistical significance in Figure 3A was achieved for cell supernatant samples treated with 25 ng/ml ($p<0.05$), 100 ng/ml ($p<0.05$), and 200 ng/ml ($p<0.001$). Figure 3B represents intracellular retention of ROS following treatment with CCL11. No statistical data was collected for this sample set due to small sample size. However, significant cell death was visible under the microscope for samples treated with 100 ng/mL and 200 ng/mL, likely contributing to the decreases seen in Figure 3B for these sample sets.

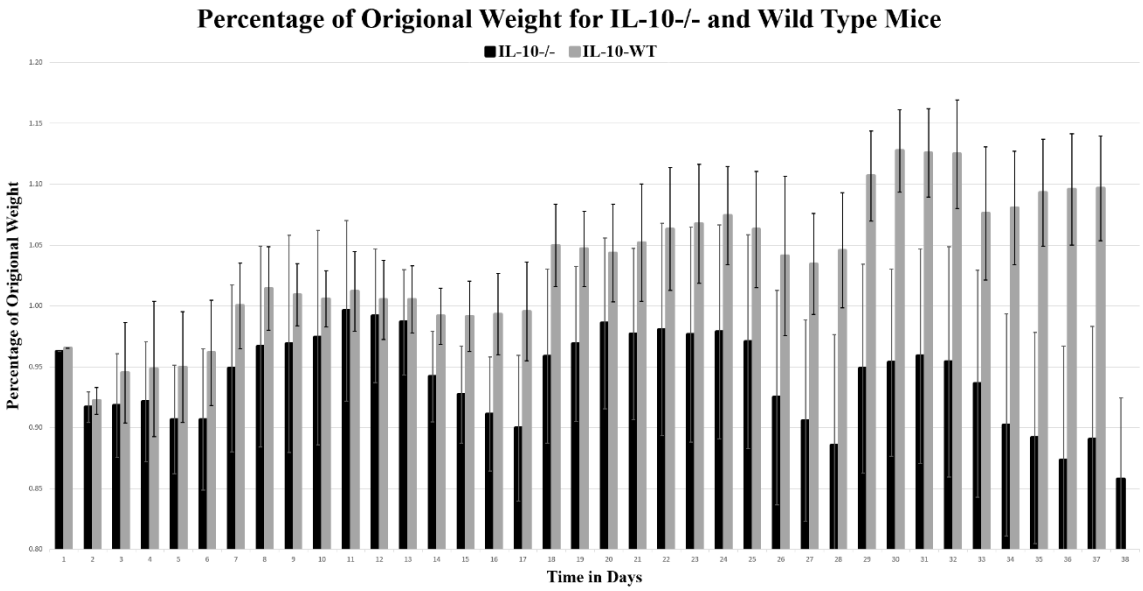

Figure 4: *Overall percentage of original weight of IL-10 -/- mice over the 38-day piroxicam experiment. Error bars signify deviation from the average.*

As depicted in Figure 4 the weights of IL-10 -/- mice were greatly influenced by the cycles of the piroxicam chow. Some mice had an increased sensitivity to the chow and did not undergo the full 3 cycles of piroxicam either due to passing before the completion of the protocol or the intervention of humane euthanasia. Even upon the reintroduction of regular chow, mice with an increased sensitivity showed little ability to recover from the treatment cycle showing increased signs of colitis through weight, rectal bleeding, and hunched posture. Mouse weights were monitored daily as a prediction of colitis with dips in weight representative of piroxicam treatment and weight gain as recovery phases between cycles. All IL-10 -/- mice ended this experiment at a lesser percentage of original weight than upon the introduction to the protocol.

Wild type weight tracking as shown in Figure 4 demonstrates a drastic difference in coping ability upon the introduction of piroxicam. Most wild type mice showed little to

no sensitivity to piroxicam with their first cycle having the greatest influence over their percentage of original weight. All wild type mice completed the experiment at a greater percentage of original weight than when they began the protocol. Observed differences in percentages of original weight between the IL-10 -/- and wild type mice speaks to the influence that the deletion of the IL-10 gene has upon the inflammatory responses within the gastrointestinal tract. IL-10 and its potent ability to ward against the induction of intestinal inflammation led to wild type mice having a much greater outcome and survival rate in counterpart to the IL-10 -/- mice which were greatly burdened by malnutrition due to intestinal inflammation.

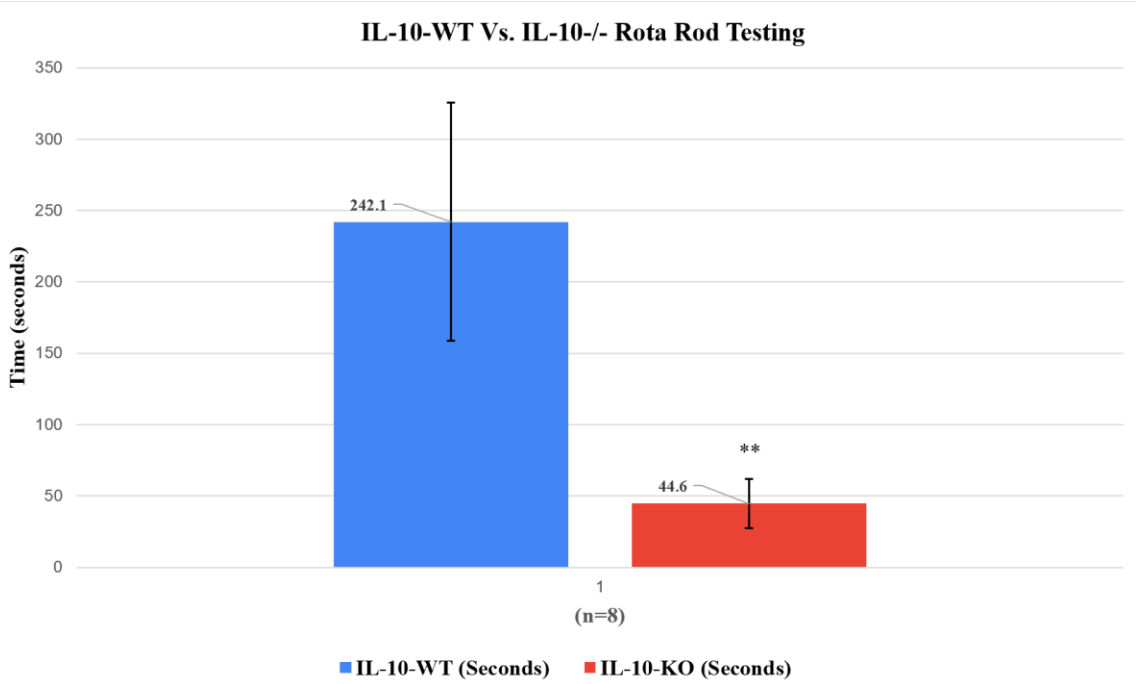

Figure 5: *Rota-Rod testing was performed on day 30 of the piroxicam experiment. Time was measured in seconds for up to 5 minutes (300 Seconds). The average of each group of mice is represented in numerical value on each bar with standard deviation represented by the error bars. P-value less than 0.05, deemed statistically significant.*

On day 30 of the piroxicam experiment all protocol mice underwent rota-rod testing for a duration of up to 300 seconds. All mice were given two trials of testing on the rota-rod and an average of all IL-10-/- mice and wild type mice is depicted in Figure 5, with error bars showing the standard deviation of each sample set. The number above each bar depicts the average of all mice in each experimental group in seconds. Wild type mice had significantly greater success during testing. Locomotor coordination and endurance was significantly greater for the wild type mice, allowing them to grip the rota-rod apparatus for ~5.4x the amount of time compared to the IL-10 -/- mice. One influence of wild type mouse success during the rota-rod test was their weight. Wild type

mice with weights greater than 30g at the time of testing had observed decreases in testing time due to increased mass influencing their ability to grip the moving bar.

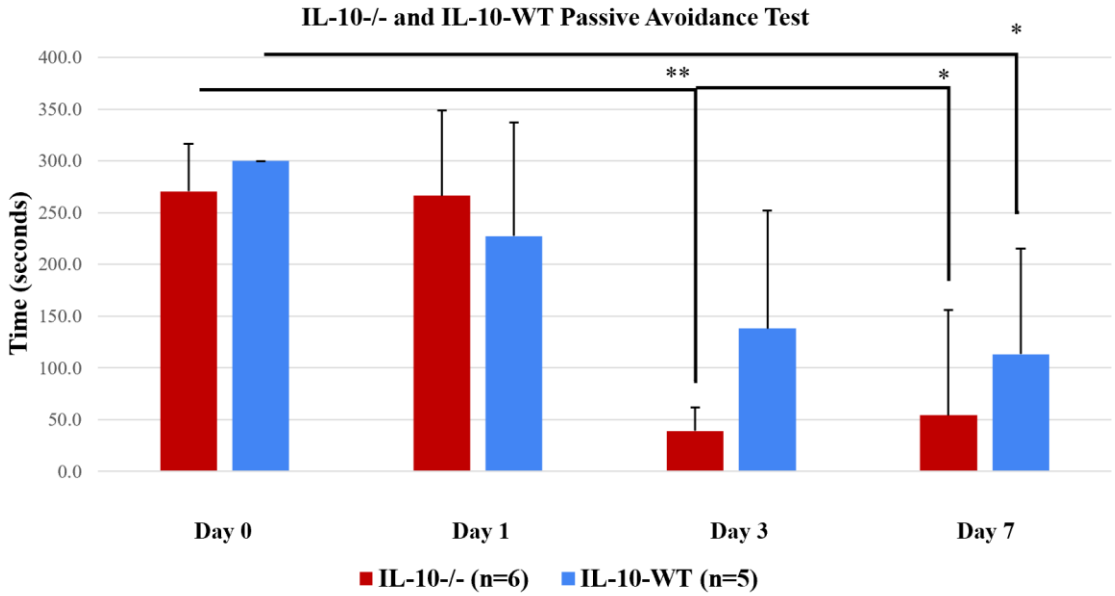

Figure 6: *Passive avoidance testing of the IL-10-KO mice (red) was initiated 24 hours after the completion of the Rota-Rod test. Mice were tested for up to 5 minutes (300 Seconds) on days 0, 1, 3, and 7. The test was ended upon all four limbs of the mouse entering the dark chamber or the completion of the test at 300 seconds. Passive avoidance testing was performed on wild-type mice (blue) following the same protocol. P-value >0.05 between IL-10-/- and wild type mice on all testing days, no statistical significance between treatment groups..*

Passive avoidance testing was performed on all protocol mice following a 24 h rest period after the rota-rod test. Over the course of seven days the memory strength of mice was assessed using passive avoidance training and testing previously outlined. Mice were maintained on regular chow diet at this time. Although no statistical difference was observed between the wild type and IL-10-/- mice, day 0 and day 1 testing was observed as having consistency in memory strength among tested mice; however, great differences were observed in the later Day 3 and Day 7 testing phases. Among the IL-10 -/- mice, as

demonstrated by the trend in Figure 6, significant reductions in memory retention of the negative stimulus were observed on Day 3 of the testing protocol. A similar reduction in memory strength was observed for the IL-10 -/- mice on Day 7. Statistical significance for the testing of the IL-10-/- mice for day 0-3 had a p-value of less than 0.001, and 0.05 for day 0-7. Wild type mice had a gradual decrease in memory strength from day 0 to day 7, demonstrating a greater retention in memory strength of the negative stimulus over the course of the test, with the only statistically significant difference being day 7 (p-value <0.05).

ANIMALS – NECROPSY OBSERVATIONS

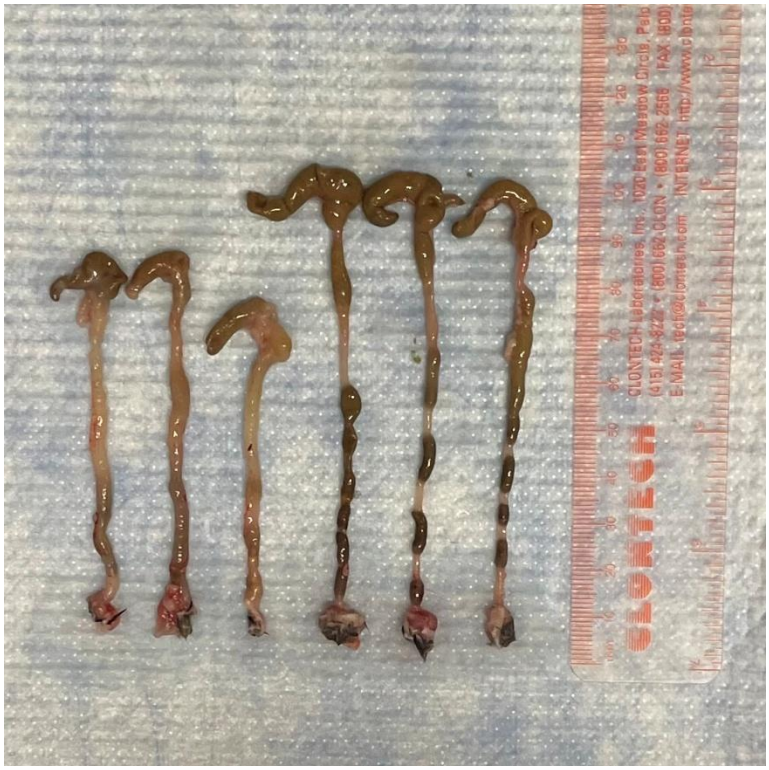

Figure 7A: *Representative image of colons harvested from IL-10-KO (left 3) and wild-type (right 3) mice. The length of the colons from each mouse was measured in mm. Colons of the IL-10-KO mice were inflamed, shortened, and had low visibility of the softer fecal matter contained within. The wild-type mice have normal colon lengths, no visible inflammation, and firm fecal matter visible within.*

Colons of all protocol mice were harvested and analyzed for visual differences between the IL-10 -/- and wild type mice. A visual representation of the harvested colons is displayed in Figure 7A, where significant shortening and inflammation was visually noted in all IL-10 -/- mice colons. Additionally, cecum size amongst the IL-10 -/- mice was smaller when compared to the wild type counterparts. Fecal matter within the colon of the IL-10 -/- mice was soft and unformed. In contrast, wild type mice had little to no intestinal inflammation and shortening, no noted shrinking of the cecum, and formed fecal matter.

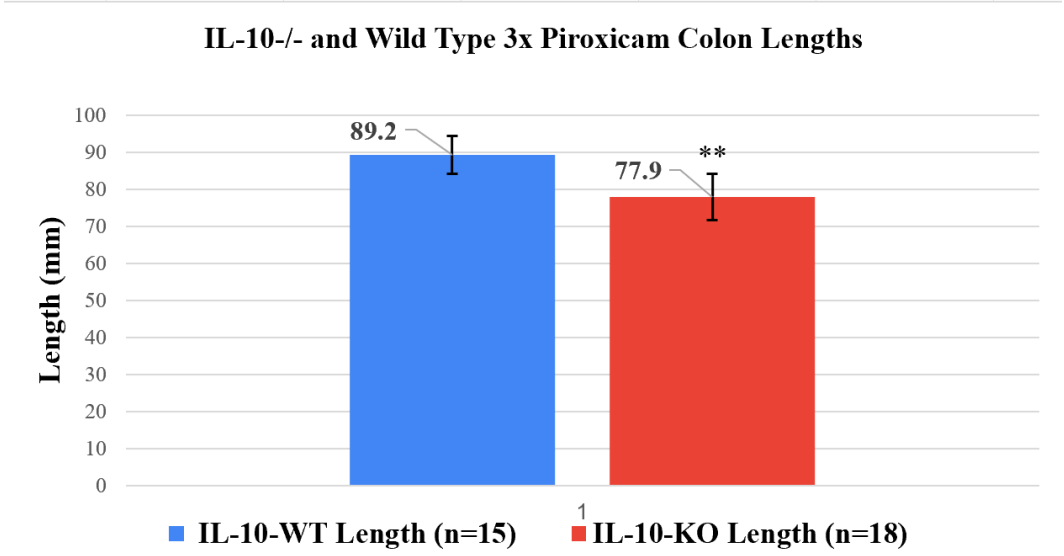

Figure 7B: *Compilation of IL-10-/- (Red) and Wild Type (Blue) colon lengths. Deemed statistically significant (P<0.001).*

Colon lengths of all 18 IL-10 -/- and 15 wild type mice are represented in Figure 7B showing a general trend in colon differences amongst the two groups. IL-10 -/- mice are represented in red and had an average colon length of 77.9 mm. Wild type mice are represented in blue and have an average colon length of 89.2 mm. Demonstrating a

significant difference amongst both groups of mice that underwent the 3x piroxicam cycle.

ANIMALS – IL-10 -/- AND WID TYPE H_2O_2 QUANTIFICATION

Quantification of H_2O_2 in the brain lysate samples of IL-10 -/- and wild type mice displays higher quantities of reactive oxygen species being present in the hippocampal regions, compared to the cerebrum samples, of both groups of mice. In the IL-10 -/- and wild type mice, hippocampal samples were ~1.6x and ~1.5 x higher than the cerebrum samples, respectively. All hippocampus and cerebrum luminescence samples were normalized using the average protein concentration of their respective sample following analysis using the Pierce™ BCA Assay Kit by Thermo Fisher Scientific™. The average of all mice in each treatment group is depicted by a corresponding value on Figure 8A and 8B. IL-10-/- mice had an average of 772.8 RLU/s in hippocampus samples and 479.0 in the cerebrum samples. Wild type mice had an average of 84.2 RLU/s in hippocampus samples and 54.4 in cerebrum samples.

In Figure 8A the hippocampus samples of the IL-10-/- and wild type mice are depicted alongside one another visually representing the ~9.2x increase in average production of H_2O_2 in the IL-10-/- hippocampus samples. Additionally, when comparing the range of each treatment group the wild type mice had a range of 18.9 – 183.6 RLU/s, in contrast to the IL-10-/- having a range of 176.7- 2538.2 RLU/s corresponding directly to the greater quantity of H_2O_2 present in sample. A similar trend is depicted by Figure 8B through the comparison of cerebrum samples which had a ~8.8x increase in average production of H_2O_2 and a range of 151.2-1237.0 RLU/s in the IL-10-/- model, in contrast to the wild type range of 0.5-174.9 RLU/s.

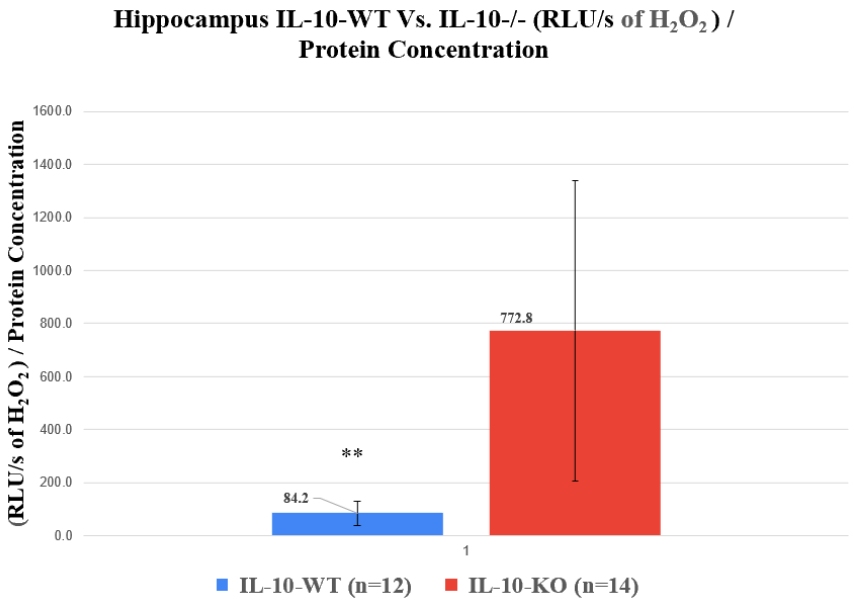

Figure 8A: *A comparison of the Hippocampus samples from the IL-10-KO and wild type mouse samples. Each sample was standardized by their protein concentration. IL-10-KO hippocampus samples are on average 9.2x higher than the wild type mice. Two-tailed p-value=7.2E-7. Deemed statistically significant (P<0.001).*

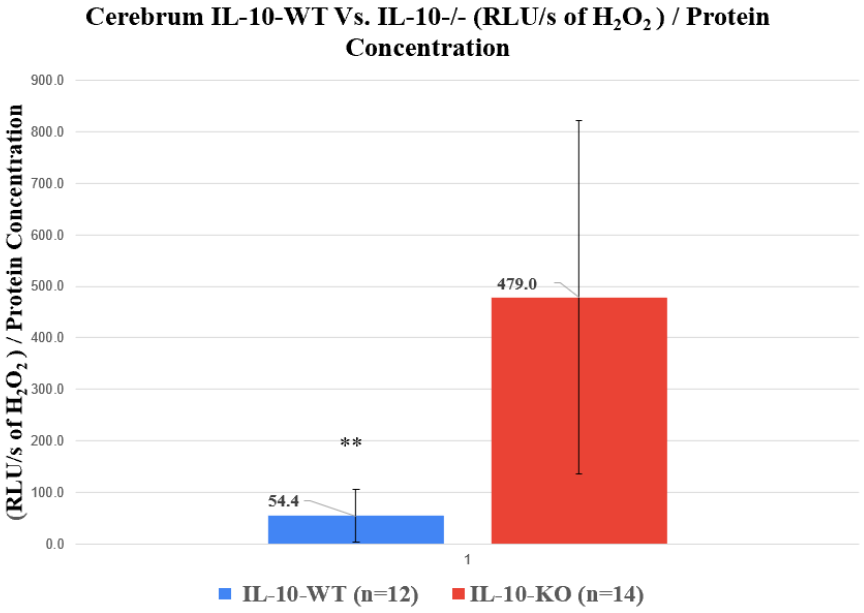

Figure 8B: *A comparison of the Cerebrum samples from the IL-10-KO and wild type mouse samples. Each sample was standardized by their protein concentration. IL-10-KO cerebrum samples are on average 8.8x higher than the wild type mice. Two-tailed p-value=5.3E-7. Deemed statistically significant (P<0.001).*

CHAPTER FOUR

DISCUSSION

IN-VITRO

We anticipated that CCL11 would induce the production of ROS in brain macrophages/microglia. CCL11 is an aging-related serum protein, with the levels of CCL11 increasing as we get older. Therefore, we suspect that CCL11-induced ROS would be linked to an increased risk of neurodegenerative diseases in seniors. With the outcome of our data, there was a notable increase in the production of H_2O_2 in both the supernatant and cell lysate samples. Supernatant samples produced statistically significant changes when comparing the control sample to that treated with 100 ng/mL and 200 ng/mL of CCL11. These results show a positive correlation between the treatment of CCL11 and the quantity of ROS released into the extracellular environment of the in-vitro SIM-A9 cells.

In in vivo models, it can be predicted that this elevated extracellular ROS would be a factor leading to decreased neurogenesis and progression of neurodegenerative processes within the brain. According to Antunes et al. (2000), due to the high permeability of H_2O_2 across the cell membrane and that most cells within the brain have lower intracellular concentrations of H_2O_2, the gradient of this compound across the cellular membrane is easily established. This means that extracellular ROS has the potential to affect neighboring tissues around where it is produced. Although cells have protective mechanisms against the damaging effects of intracellular H_2O_2, when these levels exceed that of homeostatic conditions, this compound causes oxidative stress to the cell and all intracellular components. In the research conducted for this project, it was

seen that the treatment of 100 ng/mL and 200 ng/mL caused visible cytotoxicity of the SIM-A9 cell culture under the microscope, demonstrating the effects of this potent compound on the cells that produce it, and the possible consequences of this chemokine in the death of neuronal tissues. With the significant loss of the cells stimulated by CCL11, there is the possibility that greater H_2O_2 levels could have been obtained with an increased survival rate of these stimulated cells. In vivo, microglial cells are responsible for neuronal development and maintenance. Upon stimulation with CCL11 it draws to question the ability of these cells to perform this vital function.

Through the use of the ROS-GLO^{TM} H_2O_2 Assay, proportional H_2O_2 quantification from each sample was able to be recorded in Relative Light Units. Following the calculations and protocol set forth by Promega, the distributing company, the H_2O_2 substrate was added to each sample. Upon reaction of this substrate with H_2O_2, a luciferin precursor was formed. From there the addition of ROS-GLO^{TM} Detection Solution was added to each sample promptly to produce luciferin from the precursor present in the sample. With the luciferase also present in the sample, the corresponding quantity of luciferin was able to be determined with a luminator. Due to the greater presence of luciferase in the sample, the total quantity of luciferin in each sample was recorded in RLU/s by the luminator. The RLU/s produced by each sample is directly proportional to the quantities of H_2O_2 in each sample, allowing for the quantitative analysis of the amount of ROS produced by microglial cells in response to CCL11 stimulation. Higher RLU/s values correspond to more H_2O_2 present in the sample tested. Revealing that greater stimulation of microglial cells by CCL11 corresponds to greater production and release of H_2O_2 into the extracellular environment. With the high

permeability of H_2O_2 and other superoxide species through biological membranes, the effect of ROS produced by CCL11-stimulated microglial cells likely has a great influence on surrounding tissues.

IN VIVO

Utilizing the piroxicam induced IL-10-/- colitis mouse model and wild type controls, the effects of peripheral inflammation on the brain was studied in-vivo. It is hypothesized that due to the potential for CCL11 to be up taken and retained within various regions of the brain, that CCL11 from the gastrointestinal tract would cause an increase in the production of ROS in regions of the brain where microglia are dense. This leads to a decrease in neurogenesis in these regions. The degree of colitis was tracked in the IL-10-/- and wild type mouse models using daily weight tracking, and necropsy analysis of colon inflammation and lengths at the time of euthanasia. As demonstrated by Figure 4, the IL-10-/- mice were greatly influenced upon the introduction of piroxicam chow as their diet. All IL-10-/- mice ended the three cycles of piroxicam at lesser of bodyweight percentage than that at which they entered. In contrast, the wild type mice saw the most significant impact upon the first cycle of piroxicam chow as depicted in Figure 4. Cycles two and three had contributed to minimal fluctuations in percentage of starting body weight for wild type mice, with all mice finishing the cycles of piroxicam at a greater weight than upon the introduction. It should also be noted that the survival rate for the 3 cycles of piroxicam for the IL-10-/- was 66.67% compared to the wild type 100%. Upon the completion of behavioral analysis, animals were euthanized, harvested, and necropsy analysis was completed. IL-10-/- mice had significant shortening and thickening of their colons to the point of fecal matter not being visible within the walls of

the colon as shown in Figure 7A. The wild type mice possessed colons of normal parameters with no thickening or shortening of the colonic wall. Stool encased was also well formed and easily visible in the wild type mice. Colon lengths of all harvested mice were compiled into Figure 7B, with IL-10-/- mice shown in red and wild type mice in blue. IL-10 -/- mice represented in red had an average colon length of 77.9 mm while wild type mice represented in blue had an average colon length of 89.2 mm, showing a significant difference in the length of their colons due to inflammatory responses, a key clinical hallmark of colitis. Another noted difference between the samples collected was the size of the cecum. In mice, the cecum makes up one-third of the large intestine and is largely responsible for functional fermentation (Treuting, 2011). Shrinkage of the cecum has been noted as a clinical manifestation in extreme cases of ulcerative colitis, however current data on this clinical presentation is multi-sided and inconclusive of disease outcomes (Albayrak, 2022). It should be noted that the size difference of the cecum may be due to the three cycles of piroxicam being used as the mode of colitis induction, and as an NSAID may impact the bacterial load of the cecum leading to its shrinkage.

The results from the H_2O_2 quantification demonstrated significantly higher RLU/s within the brain lysate samples of IL-10-/- mice. These values are proportional to the ROS present in samples and are standardized using the protein concentration of each individual sample. IL-10-/- mice can not combat intestinal inflammation due to the absence of their IL-10 gene, making them an ideal mouse model candidate for the study of IBD. These elevated levels within the brain demonstrate the significant link between IBD, inflammation in the gastrointestinal tract, and the consequential increase of ROS in the brain. It should also be noted that the hippocampus samples of all treated mice were

on average at least 1.5x higher than the cerebrum samples of the same mouse. This is likely due to the greater density of microglial cells, primarily responsible for producing ROS in this region of the brain (Grabert, 2016). Additionally, when comparing the mouse models as represented in Figure 8A, the hippocampus samples of the IL-10-/- mice were on average 9.2x higher than the hippocampus samples of treated wild type mice. Cerebrum samples showed a similar trend with IL-10-/- mice having an 8.8x elevation in ROS in the cerebrum samples compared to the treated wild type mice, as depicted in Figure 8B. With great quantities of ROS produced and retained within the hippocampus regions of the IL-10-/- mice, there is the great potential for damage and pathogenesis. The Hippocampus is primarily responsible for the encoding and ability to recall long term memory of people, places, objects, and events (Zelma, 2017). Damage and cognitive impairment were investigated using the rotarod and passive avoidance test. Following treatment using 3 cycles or piroxicam the mice immediately underwent rotarod testing as an evaluation of their locomotor coordination, balance, and endurance. Gait dysfunction has been associated with mild-cognitive impairment and Alzheimer's disease, with greater cognitive impairment being tied to the reduced capacity to adapt walking styles leading to increased falls (Pottorf, 2022). We hypothesized that mice inflicted by colitis would have significantly shorter timeframes on the rotarod apparatus due to the inability to adapt their gate to the moving bar. The outcomes of the rotarod testing are demonstrated in Figure 5 as datapoints representative to the time in seconds each tested mouse was able to balance on the rotarod before a fall. The average time IL-10-/- mice stayed on the rotarod apparatus was 44.6 seconds, while the wild type mice lasted on average 242.1 seconds, with mice being tested at a maximum of 300 seconds. Even with

one significant outlier, due to increased weight, wild type mice lasted on average 5.4x longer on the apparatus than the IL-10-/- mice. Showing a significant reduction in the capacity for mice with colitis to adapt their walking style, even after being trained to the rotarod apparatus.

An additional animal behavior analysis, utilized to evaluate the ability to form and retain memory, was the use of passive avoidance testing. Animals underwent training on day 0 and were naturally allowed to follow their innate instinct to enter the dark chamber. The negative stimulus was then administered for 30 seconds. A rest period of 300 seconds was then allowed before the mouse underwent day 0 testing for up to 300 seconds. Additional testing was performed on day 1, day 3, and day 7 with no negative stimulus applied at entry into the dark chamber. Day 0 and day 1 tests were performed with the desire to test short term memory retention, and day 3 and day 7 as an indicator of long-term memory. A general trend seen among tested mice is seen in Figure 6, where IL-10-/- mice demonstrated the ability to retain short term memory of the negative stimulus with timeframes in the light chamber remaining relatively even between day 0 and day 1. In comparison day 3 and day 7 saw a significant decrease in the retention of the negative stimulus leading to decreased times in the light chamber, indicating an inability to retain memory of the negative stimulus over an extended period in the IBD mouse model. Although there was not statistical significance between the IL-10-/- and wild type mice the general pattern is indicative of long-term memory loss. Wild type mice that underwent the same passive avoidance test demonstrated a greater ability to retain memory of the negative stimulus, with a more gradual decline in the retention of the negative stimulus. Although wild type mice still moved into the dark chamber, more

time in the light chamber was observed throughout all testing days, and a drastic decrease by day 7 was not as prominent. An additional mouse model used to study the impact of IBD in-vivo is the dextran sodium sulfate (DSS) mouse model utilizing C57BL/6 mice and 2.5% DSS added to their drinking water in similar 6 day on/off cycles as the piroxicam model. Although not used in this study, the DSS model can be used as an alternate model for studying IBD in-vivo.

CONCLUSIONS

Overall, the results of this study can conclude that stimulation of SIM-A9 cell cultures with CCL11 does increase the levels of ROS production by microglial cells in vitro. It also validates the ability of the ROS-GLO^{TM} H_2O_2 Assay to quantify the amount of H_2O_2 in each sample and prove the positive correlation between microglial cells, CCL11 stimulation, and ROS production. The samples stimulated with 100ng/mL and 200 ng/mL of CCL11 also demonstrated cytotoxic effects of CCL11 on microglial cells, posing potential implications of neurodegenerative disease posed by the production of CCL11 in excess. As these cells are largely responsible for neuronal health and brain homeostasis, we can also hypothesize that not only their production of ROS in the brain, but also the death of microglial cells could lead to dysfunction in neuronal health.

In vivo, inflammation in the gut led to increased levels of ROS in the hippocampus and cerebrum brain samples of IL-10-/- 3x piroxicam mice. These findings demonstrate that systemic inflammation and elevated levels of CCL11 caused by colitis can increase ROS in the hippocampus by 9.2x and cerebrum by 8.8x. Elevated levels of ROS caused by IBD have the potential to compromise neurogenesis in regions of the brain where microglial density is high, like the hippocampus, and contribute to further

neuroinflammation and cognitive decline. Animal behavioral testing demonstrated that mice with colitis had a 5.4x shorter duration on the Rota-rod apparatus compared to treated wild type mice, indicating motor coordination deficits in the colitis mice. Additionally, passive avoidance testing revealed that mice with colitis retained short term memory, but had long term memory impairment, suggesting cognitive decline due to chronic inflammation and elevated ROS in the brain.

Overall, the data supports the role of CCL11 in ROS production and subsequent microglial dysfunction, oxidative stress, and neurodegeneration. These effects are further exacerbated in the presence of systemic inflammation, as highlighted by the IBD IL-10-/- mouse model. It also depicts the potential for gut-derived chemokines like CCL11 to influence long term brain health, memory, and motor function. Although CCL11 is also an age-related chemokine, it is also greatly produced by the gastrointestinal tract in IBD cases, causing downstream oxidative effects in the brain, leading to inflammation associated neurodegenerative diseases.

LITERATURE CITED

Abdi, Z., Ivanovska, M., Macedo, D., Maes, A., Maes, M., & Murdjeva, M., (2020). CCL-11 or eotaxin-1: *An immune marker for aging and accelerated aging in neuro-psychiatric disorders*. *Pharmaceuticals, 13*(9), 230. doi:https://doi.org/10.3390/ph13090230

Ahrens, R., Ballard, B., Blanchard, C., Carey, R., Cohen, E., Denson, L., Forbes, E., Hogan, S., Lampinen, M., Lee, J,. Lee, N., Munitz, A., Rothenberg, M., Seidu, L., Stringer, K., Waddell, A., Wilson, T., & Xu, H. (2008, November 15). *Intestinal Macrophage/Epithelial Cell-Derived CCL11/Eotaxin-1 Mediates Eosinophil Recruitment and Function in Pediatric Ulcerative Colitis.* National Institutes of Health, 181(10), 7390–7399. doi: https://0.4049/jimmunol.181.10.7390

Akbar, M. D., Guillemin, G. J., Manoharan, S., Musthafa, M. E., & Rajagopal, S. A., (2016). *The role of reactive oxygen species in the pathogenesis of Alzheimer's disease, Parkinson's disease, and Huntington's disease*: A mini-review. Oxidative Medicine and Cellular Longevity. doi:https://doi.org/10.1155/2016/8590578

Albayrak, N. E., & Polydorides, A. D. (2022). Characteristics and Outcomes of Left-sided Ulcerative Colitis With a Cecal/Periappendiceal Patch of Inflammation. *The American journal of surgical pathology*, *46*(8), 1116–1125. https://doi.org/10.1097/PAS.0000000000001883

Antunes, F., & Cadenas, E. (2000). *Estimation of H_2O_2 Gradients Across Biomembranes.* FEBS Letters, 475(2), 121–126. https://doi.org/10.1016/S0014-5793(00)01638-0

Banks, W., Erickson, A., Morofuji, Y., Owen, J. (2014). *Rapid Transport of CCL11 across the Blood-Brain Barrier: Regional Variation and Importance of Blood Cells.* The Journal of Pharmacology and Experimental Therapeutics, 349 (3): 497-507. https://doi.org/10.1124/jpet.114.213074

Bassaganya-Riera, J., Eubank, S., Hontecillas, R., Wendelsdorf, K., (2010). *Model of colonic inflammation: Immune modulatory mechanisms in inflammatory bowel disease*, Journal of Theoretical Biology, 264(10), 1225-1239. https://doi.org/10.1016/j.jtbi.2010.03.027.

Carvalho, A. F., Kanchanatawan, B., Maes, M., Sirivichayakul, S., & Thika, S. (2019). *Eotaxin, an Endogenous Cognitive Deteriorating Chemokine (ECDC), Is a Major Contributor to Cognitive Decline in Normal People and to Executive, Memory, and Sustained Attention Deficits, Formal Thought Disorders, and Psychopathology in Schizophrenia Patients.* Neurotoxicity Research, 35(1), 122–138. doi:https://doi-org.huaryu.kl.oakland.edu/10.1007/s12640-018-9937-8

Çalıkuşu, A., Dağıdır, H. G., Bukan, N., & Bahçelioğlu, M. (2024). Brain-Gut Network in Inflammatory Bowel Diseases and the Role of Vagal Nerve in Neuroinflammation. *Journal of Health Science Yuksek Ihtisas University / Yüksek İhtisas Üniversitesi Sağlık Bilimleri Dergisi*, *5*(2), 66–72. https://doi.org/10.51261/yiu.2024.1442667

Culig, Z., Dal-Pont, C., Hoefer, J., Jochberger, S., Luger, M., & Schennach, H. (2017). *The "Aging Factor" Eotaxin-1 (CCL11) Is Detectable in Transfusion Blood Products and Increases with the Donor's Age*. Frontiers in Aging Neuroscience, 9(402). https://doi.org/10.3389/fnagi.2017.00402

Duellman S, Shultz J, Vidugiris G, Cali J. *A New Luminescent Assay for Detection of Reactive Oxygen Species*. Promega. 2013. Accessed October 10, 2023. https://www.promega.com/resources/pubhub/a-luminescent-assay-for-detection-of-reactive-oxygen-species/.

GBD 2021 Neurology Collaborators. (2024). Global, regional, and national burden of disorders affecting the nervous system, 1990–2021: A systematic analysis for the Global Burden of Disease Study 2021. *The Lancet Neurology, 23*(6), 545–648. https://doi.org/10.1016/S1474-4422(24)00038-3

Grabert, K., Michoel, T., Karavolos, M., Clohisey, S., Baillie, J., Stevens, M., Freeman, T., Summers, K., McColl, B. (2016) Microglial brain region−dependent diversity and selective regional sensitivities to aging. *Nat Neurosci* **19**, 504–516. https://doi.org/10.1038/nn.4222

Günther, C., Rothhammer, V., Karow, M., Neurath, M., & Winner, B. (2021). The Gut-Brain Axis in Inflammatory Bowel Disease—Current and Future Perspectives. *International Journal of Molecular Sciences*, *22*(16), 8870. https://doi.org/10.3390/ijms22168870

Guttenplan, K., & Liddelow, S. (2018, December 12) *Astrocytes and Microglia: Models and Tools.* Journal of Experimental Medicine, 216 (1): 71–83. https://doi.org/10.1084/jem.20180200

Horiuchi, H., Mizuno, T., Parajuli, B., Suzumura , A., & Takeuchi , H. (2015, July 17). *CCL11 enhances excitotoxic neuronal death by producing reactive oxygen species in microglia*. GLIA, 63(12), 2247-2248. doi:https://doi-org.huaryu.kl.oakland.edu/10.1002/glia.22892

Kim, S., Leite, G., Park, J., Pimentel, M., Rezaie, A. (2023) *Interleukin-10 Knockout Mice Do Not Reliably Exhibit Macroscopic Inflammation: A Natural History Endoscopic Surveillance Study.* Digestive Diseases and Science. 68, 1858-1862. https://doi.org/10.1007/s10620-023-07871-y

Li, M. C., & He, S. H. (2004). IL-10 and its related cytokines for treatment of inflammatory bowel disease. *World journal of gastroenterology*, *10*(5), 620–625. https://doi.org/10.3748/wjg.v10.i5.620

McDonald, W. M. (2017). *Overview of Neurocognitive Disorders*. Focus: Journal of Lifelong Learning in Psychiatry, 15(1), 4–12. https://doi.org/10.1176/appi.focus.20160030

Műzes, G., Molnár, B., Tulassay, Z., & Sipos, F. (2012). Changes of the cytokine profile in inflammatory bowel diseases. *World journal of gastroenterology*, *18*(41), 5848–5861. https://doi.org/10.3748/wjg.v18.i41.5848

Ng, S. C. (2023). Exploring the Early-Life Microbiome and Future Risk of Inflammatory Bowel Disease...Siew C. Ng. *Gastroenterology & Hepatology*, *19*(11), 693–696.

Sirivichayakul, S., Kanchanatawan, B., Thika, S., Carvalho, A. F., & Maes, M. (2019). *Eotaxin, an Endogenous Cognitive Deteriorating Chemokine (ECDC), Is a Major Contributor to Cognitive Decline in Normal People and to Executive, Memory, and Sustained Attention Deficits, Formal Thought Disorders, and Psychopathology in Schizophrenia Patients.* Neurotoxicity Research: Neurodegeneration, Neuroregeneration, Neurotrophic Action, and Neuroprotection, 35(1), 122–138. https://doi.org/10.1007/s12640-018-9937-8

Pottorf, T. S., Nocera, J. R., Eicholtz, S. P., & Kesar, T. M. (2022). Locomotor Adaptation Deficits in Older Individuals With Cognitive Impairments: A Pilot Study. *Frontiers in neurology*, *13*, 800338. https://doi.org/10.3389/fneur.2022.800338

Song, Z., Li, X., Xie, J., Han, F., Wang, N., Hou, Y., & Yao, J. (2024). Associations of inflammatory cytokines with inflammatory bowel disease: a Mendelian randomization study. *Frontiers in immunology*, *14*, 1327879. https://doi.org/10.3389/fimmu.2023.1327879

Treuting, P., & Dintzis, S. (2011, November 23). *Lower Gastrointestinal Tract*. Comparative Anatomy and Histology. https://doi.org/10.1016/B978-0-12-381361-9.00012-3

Zemla, R., & Basu, J. (2017). Hippocampal function in rodents. *Current opinion in neurobiology*, *43*, 187–197. https://doi.org/10.1016/j.conb.2017.04.005

Zhang, B., Wang, H. E., Bai, Y. M., Tsai, S. J., Su, T. P., Chen, T. J., ... Chen, M. H. (2021). Inflammatory bowel disease is associated with higher dementia risk: A nationwide longitudinal study. *Gut, 70*(1), 85–91. https://doi.org/10.1136/gutjnl-2020-320789

Zhu, Y., Yuan, M., Liu, Y., Yang, F., Chen, W.-Z., Xu, Z.-Z., Xiang, Z.-B., & Xu, R.-S. (2022). Association between inflammatory bowel diseases and Parkinson's disease: A systematic review and meta-analysis. *Neural Regeneration Research, 17*(2), 344–353. https://doi.org/10.4103/1673-5374.317981

APPENDIX

OAKLAND UNIVERSITY
Powered by Google

Sang Hoon Rhee <srhee@oakland.edu>

Committee Action Record – IACUC Protocol # 2022-1183 Amendment Approval

eSirius3GWebServer <no-reply@esirius.cayuse.com> Tue, Aug 27, 2024 at 7:41 AM
To: srhee@oakland.edu

cayuse Animal Oversight

Reference: IACUC Protocol # 2022-1183

Protocol Title: The Study of Gastrointestinal Pathobiology

Principal Investigator: Rhee, Sang Hoon

Approval Period: 10/04/2023 - 10/04/2026

Dear Professor Rhee, Sang Hoon:

The Institutional Animal Care and Use Committee (IACUC) has reviewed the amendment to protocol number 2022-1183, noted the required modifications provided by you upon committee's request (if applicable), and approved the project amendment referenced above. The reason for the amendment is:

- Adding the Procedures 16 and 17 for CYD19 administration in mice

The amended protocol retains the original approval period (starting 10/04/2023 and ending 10/04/2026) and assigned application # 2022-1183. This is your formal approval notice; please save it for your records. Be aware that protocols expire at 12:01 AM on the expiration date. Ninety (90) days before the protocol approval expires, Cayuse will send you an alert email prompting you to submit a De Novo application to renew the project, if desired. Any unanticipated problems, changes in, or halting of the activities proposed in the project, as described, must be promptly reported to the IACUC Administrator.

In addition, all faculty, staff, and students involved in the project must be trained and qualified to conduct the project in a responsible manner. Please note, in this regard, that you, the Principal Investigator, are fully responsible at all times.

Please let me know if you have any questions.

Sincerely,

Rick Marble
Animal Research Facility Manager and IACUC Administrator

(email ID #400014)

*** THIS IS AN EMAIL NOTIFICATION ONLY. PLEASE DO NOT REPLY ***